

OMTO, Volume 20

Supplemental Information

Single-cell RNA-sequencing analyses identify heterogeneity of CD8⁺ T cell subpopulations and novel therapy targets in melanoma

Weiwei Deng, Yubo Ma, Zhen Su, Yufang Liu, Panpan Liang, Chen Huang, Xiao Liu, Jin Shao, Yi Zhang, Kai Zhang, Jian Chen, and Ruoyu Li

Supplementary materials

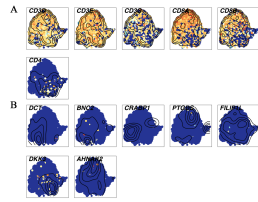


Figure S1. t-SNE plots of marker genes were used to verify the accuracy of CD8⁺ T cells.

The single-cell transcript levels of T cell markers (*CD3D*, *CD3E*, *CD3G*), CD8⁺ T cell markers (*CD8A*, *CD8B*), and CD4⁺ T cell markers (*CD4*) (A). The single-cell transcript levels of melanocyte markers (*DCT*, *BNC2*, *CRABP1*, *PTGDS*, *FILIP1L*, *DKK3*, *AHNAK2*) (B).

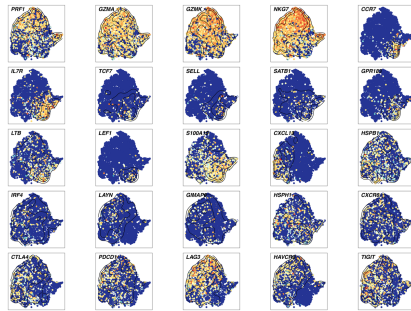


Figure S2. Single-cell transcript levels of signature genes.

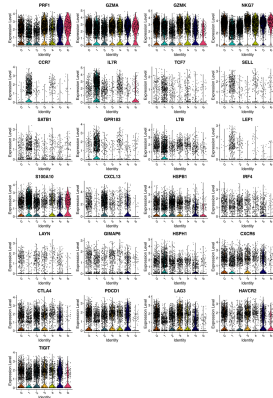


Figure S3. Violin plots of signature genes across each subpopulation.

Colors of violin plots correspond with annotated subpopulations in Figure 1(E-F).

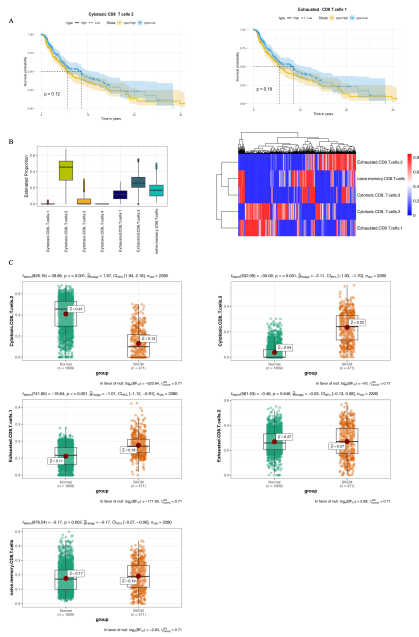


Figure S4. Frequency of CD8⁺ T cell subpopulations in normal samples.

(A) No significant difference for cytotoxic subpopulation 2 and exhausted subpopulation 1 in SKCM prognoses. (B) Proportions of CD8⁺ T cell subpopulations in normal samples. (C) Differential analysis of CD8⁺ T cell subpopulations between SKCM and normal samples.

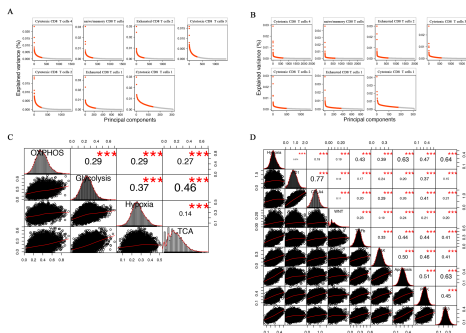


Figure S5. The results of PCs variation and relationships between hypoxia and other pathways.

(A-B) PCs variation from PCA based on metabolic gene transcript levels (A) and hallmark gene express levels. Red represented top 80% PCs variation. (C-D) The correlations between hypoxia and metabolic pathways (C), and the relationship between hypoxia and hallmark pathways (* $p < 0.05$; ** $p < 0.01$; *** $p < 0.001$).

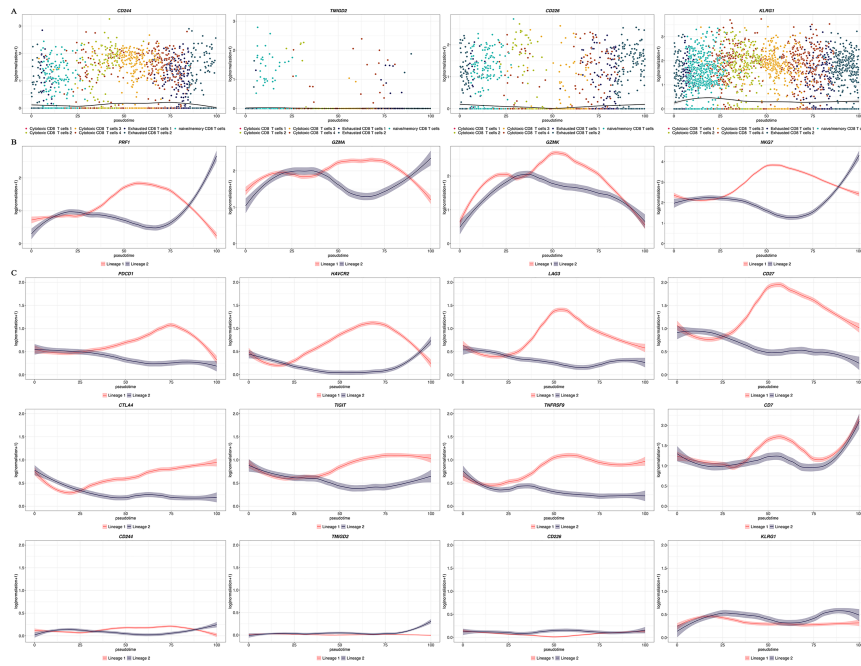


Figure S6. Expression profiles of cytotoxic and immune checkpoint molecules.

(A) Immune checkpoints without changes in lineage 1. (B-C) Transcript profiles of cytotoxic genes (B) and immune checkpoints (C) within lineage 1 and lineage 2.

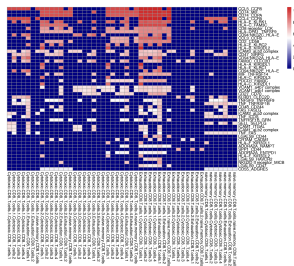


Figure S7. A heatmap showed the distribution of ligand-receptor pairs among different subpopulations.

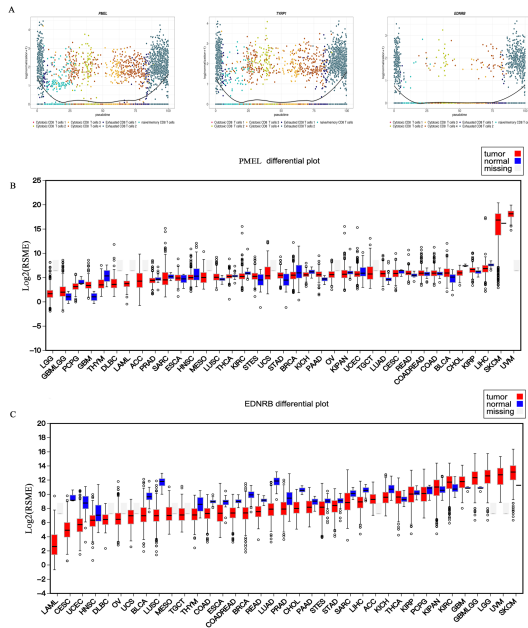


Figure S8. Expression levels of *PMEL*, *TYRP1*, and *EDNRB*.

(A) Transcript profiles of *PMEL*, *TYRP1*, and *EDNRB* in lineage 1. (B-C) The expression values of *PMEL* (B) and *EDNRB* (C) across 37 tumors and normal samples (download from FIREBROWSE database).

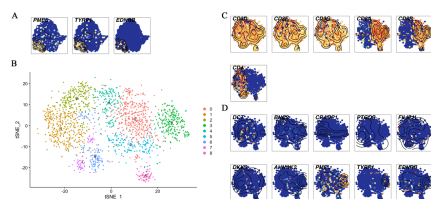


Figure S9. Expression levels of *PMEL*, *TYRP1*, and *EDNRB* in single cells and different datasets.

(A) Single-cell transcript levels of *PMEL*, *TYRP1*, and *EDNRB* ($CD8^+$ T cells were classified by us). (B) The t-SNE plots for T cells. (C) The single-cell transcript levels of T cell markers (*CD3D*, *CD3E*, *CD3G*), $CD8^+$ T cell markers (*CD8A*, *CD8B*), and $CD4^+$ T cell markers (*CD4*). (D) The single-cell transcript levels of melanocyte markers (*DCT*, *BNC2*, *CRABP1*, *PTGDS*, *FILIP1L*, *DKK3*, *AHNAK2*) and the novel targets (*PMEL*, *TYRP1*, *EDNRB*). (B-D) T cells were classified by Tirosh et al., and we used the data to validate the expression levels of *PMEL*, *TYRP1*, and *EDNRB*.